arXiv:1110.3769v1 [astro-ph.CO] 17 Oct 2011

Cepheid Period-Luminosity Relations in the Near-Infrared and the Distance to M31 from the Hubble Space Telescope Wide Field Camera 3 *

Adam G. Riess[1,2], Jürgen Fliri[3] and David Valls-Gabaud[3]

ABSTRACT

We present measurements of 68 classical Cepheids with periods from 10 to 78 days observed in the near-infrared by the PHAT Program using the Wide Field Camera 3 (WFC3) on the *Hubble Space Telescope (HST)*. The combination of HST's resolution and the use of near-infrared measurements provides a dramatic reduction in the dispersion of the Period–Luminosity relation over the present optical, ground-based data. Even using random-phase magnitudes we measure a dispersion of just 0.17 mag, implying a dispersion of just 0.12 mag for mean magnitudes. The error in the mean for this relation is 1% in distance. Combined with similar observations of Cepheids in other hosts and independent distance determinations, we measure a distance to M31 of $\mu_0 = 24.42 \pm 0.05(statistical) \pm 0.03(systematic)$, 765 ± 28 kpc, in good agreement with past measurements though with a better, 3% precision here. The result is also in good agreement with independent distance determinations from two detached eclipsing binaries allowing for an independent calibration of the Cepheid luminosities and a determination of the Hubble constant.

Subject headings: cosmology: observations — cosmology: distance scale — galaxies: distances and redshifts — stars: variables: Cepheids — cosmological parameters

1. Introduction

M31, the nearest analogue of the Milky Way Galaxy, has long provided important clues to understanding the scale of the Universe. The naked-eye visibility in 1885 of a supernova in M31 (S And, see De Vaucouleurs & Corwin 1985) once suggested the spiral nebulae were located within the Milky Way lest its luminosity be "*on a scale of magnitude such as the imagination recoils from*

*Based on observations with the NASA/ESA *Hubble Space Telescope*, obtained at the Space Telescope Science Institute, which is operated by AURA, Inc., under NASA contract NAS 5-26555.

[1]Department of Physics and Astronomy, Johns Hopkins University, Baltimore, MD 21218.

[2]Space Telescope Science Institute, 3700 San Martin Drive, Baltimore, MD 21218; ariess@stsci.edu

[3]LERMA, CNRS UMR 8112, Observatoire de Paris, 61 Avenue de l'Observatoire, 75014 Paris, France; jurgen.fliri@obspm.fr, david.valls-gabaud@obspm.fr

contemplating" (Clerke 1903). Hubble's (1929) subsequent discovery of Cepheid variables in M31 revealed the true gulf that existed between the Milky Way and other galaxies. The ability to resolve the stellar populations of M31 and knowledge of its distance still provides the best constraints on the timescales of the formation of such massive galaxies (Brown et al. 2006). Despite long past success in identifying Cepheids in M31 (Baade & Swope 1963, 1965), comprehensive inventories of its variables were not completed until the availability of wide-format CCD arrays to survey its 3 degree span and image-subtraction techniques to contend with the extreme crowding of its stars, a consequence of its 77° inclination. Large-scale variability surveys in the 1990s by Magnier et al. (1997), the DIRECT Program (e.g. Bonanos et al. 2003), and Vilardell et al. (2007), as well as microlensing surveys in the 2000s, by POINT-AGAPE (An et al. 2004) and WeCAPP (Fliri et al. 2006), succeeded in discovering $\sim 10^3$ Cepheids, most from > 50 Myr-old supergiants at short periods ($P < 10$ days). The Pixel Observations of M31 with MEgacam (POMME) survey has been the most prolific to date, making use of Megacam on CFHT to discover more than 2500 Cepheids (Fliri et al. 2012).

The utility of Cepheids as distance indicators critically depends on the accuracy of their measured fluxes. Even the best optical measurements of M31 Cepheids from the ground have been biased bright at the $0.1 - 0.2$ mag level by stellar crowding (Mochejska et al. 2000; Vilardell et al. 2007) and contaminated by variable extinction owing to the high inclination of its host. Space-based observations in the near-infrared have the ability to greatly mitigate both of these sources of error. A modest sample of 8 Cepheids in M31 was measured with greater resolution and in the near-infrared using the NICMOS Camera on the Hubble Space Telescope (HST) by Macri et al. (2001), suggesting that both crowding and extinction could be tamed by such measurements.

The Panchromatic Hubble Andromeda Treasury (PHAT) Program (P.I. J. Dalcanton) is a Hubble Space Telescope Multi-cycle Treasury program to map roughly a third of M31's star forming disk, using 6 filters covering from the ultraviolet through the near-infrared. With HST's resolution and sensitivity, the disk of M31 will be resolved into more than 100 million stars, enabling a wide range of scientific endeavors. Despite capturing only a static view of M31, the random phase observations of known Cepheids obtained by PHAT are nearly as precise as mean phase observations for measuring the distance to M31 due to the small amplitudes of Cepheid light curves in the near-infrared (Madore & Freedman 1991). Because the Cepheid observations are obtained with the same near-infrared photometric system as recent distance scale data (Riess et al. 2011), the PHAT observations provide the means to determine the distance to M31 with lower systematic error than past estimates. The recent discovery and characterization of detached eclipsing binary sytems (DEB) in M31 (Ribas et al. 2005; Vilardell et al. 2010) offers reliable and independent distance determinations to M31 which can be used to calibrate Cepheid luminosities and ultimately the Hubble constant. These measurements are also valuable for characterizing the slope of the period-luminosity relation at solar metallicity at long-periods in the same near-infrared band used to determine the Hubble constant (Riess et al. 2011).

We have analyzed the first year of PHAT data to locate and measure the long-period Cepheids

($\log P(\mathrm{day}) > 1$) previously discovered by image-subtraction in ground-based variability surveys, mostly from POMME. In Section 2 we present images of the recovered long-period Cepheids from the PHAT survey and their near-infrared photometry. In Section 3 we analyze this data to constrain the distance to M31, the slope of the P–L relation in $F160W$ and its impact on the Hubble constant.

2. WFC3 Observations of Cepheids in M31

The PHAT program (Dalcanton & et al. 2012) is imaging the northeast quadrant of M31 with WFC3 with 2 UV filters ($F275W$, $F336W$), 2 IR filters ($F110W$, $F160W$) and 2 optical filters with ACS ($F475W$, $F814W$) over the course of a 3 year survey. All WFC3 images are collected in a single epoch with those from ACS obtained approximately 6 months before or after the WFC3 images when the orientation of HST allows overlapping coverage in parallel. We searched the PHAT data for Cepheids with $\log P > 1$ as these match the period range of Cepheids observed by HST at > 20 Mpc used in studies of the distance scale. Our primary source of positions and periods of Cepheids was the recent POMME Survey from Megacam on CFHT whose sample of > 2500 Cepheids covering most of M31 is the largest sample collected to date (Fliri et al. 2012), with 180 in the North half of M31 with $\log P > 1$. While many of the Cepheids found in previous surveys are included in the POMME sample, the reverse is not true. We also consulted the variability catalog from the DIRECT program (Bonanos et al. 2003) to search for additional long-period Cepheids not included in the POMME sample. In the first year PHAT obtained data through the middle of 2011, and 65 long-period POMME Cepheids were contained in the survey, a fair fraction of the ~ 90 likely to be imaged by the end of the Survey. These 65 were augmented with 1 object from DIRECT and 2 from the Pan-STARRS survey data (Lee et al. 2011).

Precise positions of the Cepheids in the HST images of M31 were determined by refining steps in the relative astrometry between ground- and space-based imaging. The ground-based survey positions were first used to identify the approximate region hosting the Cepheids in the HST images to $\sim 0\farcs4$ precision, with the uncertainty resulting from the HST guide star position errors. Next, a geometric transformation was defined by matching unresolved sources in $20''$ diameter regions in the ground-based i-band POMME data and the WFC3 $F110W$ images. The derived transformations were used with the POMME Cepheid coordinate to locate the Cepheid positions to within one WFC3-IR pixel ($\sigma{\sim}0\farcs1$). For a few Cepheids with close neighbors, identifications of the Cepheids in the $F336W$ images were used to confirm the Cepheid position among neighboring red giants (missing in the UV) or luminous blue dwarves (missing in the IR). Lastly, centroids for the Cepheids in the HST images were measured together with photometry resulting in the positions given in Table 1. The high signal-to-noise ratio of the Cepheid data in the HST images (SNR $>$ 100) and minimal crowding (see Figure 1) insures negligible bias in the measured positions.

Table 1. M31 Cepheids in WFC3-IR

α (J2000)	δ (J2000)	Id[a]	P (day)	$F160W^b$ (mag)	$F110W$ (mag)	Bias (mag)	[O/H] zkh
10.896242	41.258875	vn.5.1.1120	12.95	18.78 (0.05)	19.09 (0.09)	0.009	9.008
11.202987	41.487450	vn.3.1.518	14.18	18.25 (0.03)	18.42 (0.06)	0.003	8.948
11.235392	41.472761	vn.3.1.357	21.73	18.11 (0.03)	18.62 (0.07)	0.002	8.922
11.200633	41.449286	vn.3.1.535	21.03	18.05 (0.03)	18.54 (0.06)	0.003	8.930
11.209271	41.452631	vn.3.1.484	15.54	18.46 (0.03)	18.98 (0.08)	0.004	8.927
11.182408	41.476428	vn.3.1.663	14.69	18.53 (0.03)	18.99 (0.08)	0.002	8.954
11.185921	41.417044	vn.3.1.622	12.56	18.67 (0.03)	19.04 (0.08)	0.002	8.922
11.131458	41.632081	vn.4.2.246	13.24	18.55 (0.03)	18.83 (0.07)	0.004	9.028
11.138413	41.626025	vn.4.2.197	10.62	18.54 (0.03)	18.84 (0.07)	0.008	9.025
11.091775	41.664158	vn.4.2.508	10.87	18.87 (0.03)	19.22 (0.09)	0.004	9.033
11.038733	41.662008	vn.4.2.849	13.36	18.61 (0.03)	18.88 (0.08)	0.008	9.034
11.039342	41.659111	vn.4.2.845	12.31	18.50 (0.03)	18.65 (0.07)	0.012	9.035
11.129060	41.613420	vn.4.2.268	12.32	18.45 (0.03)	18.75 (0.07)	0.004	9.027
11.046342	41.654658	vn.4.2.781	11.23	18.87 (0.03)	19.09 (0.08)	0.000	9.037
11.096287	41.588286	vn.4.2.480	12.91	18.48 (0.03)	18.64 (0.07)	0.002	9.035
10.953500	41.624042	vn.5.2.475	18.61	17.95 (0.03)	18.44 (0.06)	0.004	9.035
10.965058	41.620431	vn.5.2.390	12.47	18.46 (0.03)	18.80 (0.07)	0.008	9.040
10.972425	41.631158	vn.5.2.333	10.73	18.71 (0.04)	18.88 (0.08)	0.004	9.036
11.348500	41.693375	vn.2.2.497	36.16	17.34 (0.03)	17.93 (0.05)	0.001	8.952
11.354621	41.708811	vn.2.2.463	16.55	18.62 (0.03)	18.74 (0.07)	0.003	8.953
11.363342	41.699800	vn.2.2.408	28.70	17.62 (0.03)	18.04 (0.05)	0.001	8.946
11.368488	41.659503	vn.2.2.378	10.60	19.15 (0.03)	19.30 (0.09)	0.008	8.930
11.377304	41.657669	vn.2.2.340	15.51	18.24 (0.03)	18.53 (0.06)	0.002	8.925
11.326300	41.650592	vn.2.2.647	12.50	19.00 (0.03)	19.32 (0.09)	0.003	8.948
11.331008	41.666139	vn.2.2.616	14.12	18.34 (0.03)	18.57 (0.06)	0.002	8.951
11.276512	41.694817	vn.3.2.299	10.03	18.79 (0.03)	19.06 (0.08)	0.004	8.984
11.279687	41.621742	vn.3.2.272	26.46	17.75 (0.03)	17.99 (0.05)	0.000	8.962
11.332550	41.788881	vn.2.3.463	11.14	18.78 (0.03)	19.10 (0.08)	0.006	8.976
11.421142	41.747228	vn.2.2.158	11.62	18.77 (0.03)	19.11 (0.08)	0.001	8.933
11.308658	41.764531	vn.3.3.41	12.75	18.51 (0.03)	18.70 (0.07)	0.003	8.982
11.351142	41.735061	vn.2.2.492	20.17	18.01 (0.03)	18.31 (0.06)	0.001	8.961
11.354621	41.708811	vn.2.2.463	16.55	18.62 (0.03)	19.01 (0.08)	0.003	8.953
11.343588	41.903383	vn.2.3.425	13.04	18.54 (0.03)	18.89 (0.08)	0.004	8.968
11.266917	41.933294	vn.3.3.237	18.79	18.09 (0.03)	18.60 (0.07)	0.000	8.957
11.184892	41.927108	vn.3.3.945	10.30	19.04 (0.03)	19.26 (0.09)	0.008	8.944

Table 1—Continued

α (J2000)	δ (J2000)	Id[a]	P (day)	$F160W$[b] (mag)	$F110W$ (mag)	Bias (mag)	[O/H] zkh
11.331612	41.886650	vn.2.3.468	22.15	18.05 (0.03)	18.37 (0.06)	0.002	8.972
11.154013	41.876450	vn.4.3.114	11.47	19.07 (0.04)	19.22 (0.09)	0.001	8.962
11.163267	41.881942	vn.4.3.54	13.88	18.68 (0.03)	19.10 (0.08)	0.002	8.961
11.143313	41.911761	vn.4.3.181	13.54	18.34 (0.03)	18.63 (0.07)	0.000	8.941
11.345917	41.845825	vn.2.3.413	16.38	18.35 (0.03)	18.70 (0.07)	0.002	8.974
11.282308	41.854561	vn.3.3.173	18.92	18.26 (0.03)	18.56 (0.06)	0.002	8.982
11.303358	41.829725	vn.3.3.77	12.83	18.76 (0.03)	19.05 (0.08)	0.002	8.983
11.307717	41.849969	vn.3.3.54	35.91	17.24 (0.03)	17.68 (0.04)	0.001	8.980
11.231963	41.865203	vn.3.3.731	11.18	18.71 (0.03)	18.91 (0.08)	0.004	8.979
11.098375	41.863444	vn.4.3.420	14.66	18.30 (0.03)	18.70 (0.07)	0.002	8.953
11.111754	41.843253	vn.4.3.353	20.23	17.92 (0.03)	18.10 (0.05)	0.002	8.967
11.445392	41.912014	vn.2.3.69	14.64	18.29 (0.03)	19.03 (0.08)	0.001	8.949
11.410238	41.903642	vn.2.3.203	10.97	19.05 (0.03)	19.50 (0.10)	0.004	8.958
11.415517	41.910472	vn.2.3.178	11.15	18.79 (0.03)	19.07 (0.08)	0.001	8.956
11.455404	41.864358	vn.2.3.21	16.12	18.54 (0.03)	18.81 (0.07)	0.002	8.943
11.380758	41.880753	vn.2.3.314	10.43	18.98 (0.03)	19.28 (0.09)	0.006	8.965
11.381112	41.853336	vn.2.3.311	31.61	17.44 (0.03)	17.83 (0.04)	0.001	8.965
11.367142	41.837386	vn.2.3.354	24.20	17.67 (0.03)	18.22 (0.05)	0.003	8.969
11.375225	41.817983	vn.2.3.333	17.29	18.71 (0.03)	19.22 (0.09)	0.003	8.965
11.394033	41.828908	vn.2.3.260	14.93	18.11 (0.03)	18.45 (0.06)	0.002	8.960
11.393396	41.937289	vn.2.3.265	15.34	18.28 (0.03)	18.69 (0.07)	0.004	8.957
11.243525	41.945469	vn.3.3.325	28.61	17.45 (0.03)	17.80 (0.04)	0.001	8.949
11.576296	42.216006	vn.1.4.92	10.97	19.29 (0.03)	19.68 (0.11)	0.000	8.884
11.575821	42.184472	vn.1.4.93	12.33	18.79 (0.03)	19.24 (0.09)	0.000	8.893
11.450667	42.214064	vn.2.4.28	21.15	18.20 (0.03)	18.43 (0.06)	0.000	8.869
11.464258	42.140753	vn.2.4.2	10.22	18.69 (0.03)	18.96 (0.08)	0.000	8.901
11.169900	41.903150	091-2412	17.45	18.02 (0.03)	18.43 (0.06)	0.002	8.952
11.064200	41.569270	vn.4.2.678	78.00	16.07 (0.03)	16.50 (0.02)	0.001	9.044
10.985150	41.217580	vs.1.4.439	17.57	18.05 (0.03)	18.38 (0.06)	0.002	8.930
10.929470	41.247570	D31.D.836	41.79	16.83 (0.03)	17.30 (0.03)	0.000	8.981
10.918150	41.185690	vs.2.4.272	55.79	17.08 (0.03)	17.52 (0.04)	0.000	8.951
10.952310	41.153930	vs.2.4.41	20.29	17.83 (0.03)	18.12 (0.05)	0.002	8.911
10.810760	41.504040	078-1587	21.67	18.01 (0.03)	18.42 (0.06)	0.004	9.054

[a]Source of optical parameters for the Cepheids: vn*/vs* POMME (Fliri et al. 2012), 0* (Pan-STARRS); D* DIRECT (Bonanos et al. 2003)

[b] includes absolute zeropoint uncertainty of 0.03 mag

Table 2. PLCZ Fits to M31 Cepheids

Relation	Band	σ	b	$\delta M/\delta$[O/H]	$m(\log P = 1.2)$
PL	$F160W$	0.174	-3.003 (0.127)		18.292 (0.021)
PL	$F110W$	0.201	-2.725 (0.150)		18.637 (0.024)
PLW	$F160W, F110W$	0.216	-3.432 (0.167)		17.761 (0.026)
PLW	$F160W, F336W$	0.195	-3.433 (0.145)		17.639 (0.024)
PLCZ	$F160W, F110W$	0.214	-3.419 (0.160)	-0.65 (0.73)	17.761 (0.026)

The $F160W$ images for each pointing, consisting of 1600 s in 4 dithered exposures, were combined and resampled to a final scale of $0\farcs08$ pixel^{-1}. The Cepheid photometry was measured by simultaneously fitting model PSFs to the Cepheid and any unresolved sources in its vicinity using the same zeropoint scale derived from the standard star P330E as in Riess et al. (2011). Artificial stars were added to the images and measured to assess the crowding bias and to determine the photometric errors. The mean bias was 0.002 mag and the mean statistical error was 0.01 mag. With the $F110W$ filter, only a single dither of 700 or 800 s was obtained limiting the value of resampling the image on a finer scale and the use of PSF fitting, so we measured the $F110W$ flux in small apertures of 2 pixel radius. Cepheid parameters are given in Table 1.

The $F160W$ and $F110W$ P–L relations are shown in Figure 2 with relevant parameters in Table 2. For historical interest, we have included one additional measurement in Figure 2, the HST WFC3-IR $F110W$ observation of Hubble's (1929) first Cepheid discovered in M31, V1 with $P = 31.4$ days, observed by his namesake telescope by the Hubble Treasury Program Team (P.I. K. Noll). The fitted slope of -3.00 ± 0.13 for $F160W$ is in good agreement with the value of -2.91 ± 0.06 found for 448 more distant Cepheids in 9 hosts with the same filter and instrument (Riess et al. 2011). The M31 slope is about 1.5 σ shallower than the slope of -3.20 ± 0.06 we estimate for the LMC Cepheids from Persson et al. (2004) after interpolating between the ground-based J- and H-band slopes. The dispersion of the M31 Cepheids about this relation, 0.17 mag, is a factor of 3.5 times lower than that of the optical P–L relations measured for M31 from the ground and even less than the 0.23 mag dispersion measured by Macri et al. (2001) with NICMOS, likely a result of the greater photometric stability of WFC3-IR. Although the dispersion is larger than the 0.13 mag dispersion measured by Persson et al. (2004) in the H-band in the LMC, the difference is readily explained by our use of random phase measurements. Resampling random phases from the Persson et al. (2004) light curves yields an average dispersion of 0.18 mag with no offset, a result nearly identical to ours, and confirming a similar intrinsic dispersion of 0.12 mag. A slope-insensitive distance indicator for our sample, the mean Cepheid magnitude at the sample mean period of $\log P = 1.2$, is 18.292 ± 0.021 mag, sufficient to measure the distance to M31 to 1% given sufficient calibration.

The dispersion increases to 0.20 mag for $F110W$. While some of the increase may result from additional differential extinction, most appears to come from the larger amplitudes of the light curves at shorter wavelengths. The LMC Cepheids predict a random phase dispersion of 0.22 mag. A strong correlation between the IR band residuals is apparent in Figure 2, as expected from our use of random but coincident phases as well as from intrinsic variation.

Next we fit a Wesenheit relation (PLW in Table 2) to account for the effect of differential extinction along the inclined line of sight of the form $F160W - 1.54(F110W - F160W) = a + b \log P$ where 1.54 is the value of A_{F160W} per magnitude of $A_{F110W} - A_{F160W}$ for a Cardelli et al. (1989) reddening law with $R_V = 3.1$. The slope of this fit, -3.43 ± 0.17, is in good agreement with the slope of -3.38 ± 0.09 for the same relation in J and H for the LMC (Persson et al. 2004). A similar result was found using the $F336W$ UV color in place of $F110W$ with a reddening term of 0.14. Next

we included a metallicity parameter (PLCZ in Table 2) to account for any apparent correlation between Cepheid near-infrared fluxes and the local value of $12 + \log[O/H]$ measured from HII regions, a proxy for Cepheid metallicity. Use of the deprojected radial gradient from Zaritsky et al. (1994) results in an insignificant correlation of -0.65 ± 0.73 mag per dex, compared to -0.10 ± 0.09 mag per dex from the extragalactic Cepheids in Riess et al. (2011). The M31 Cepheids have little grasp on the Cepheid metallicity parameter because they lie in a narrow annulus along the disk (Fliri et al. 2012) with a full range of less than 0.2 dex ($12 + \log[O/H]$=8.87 to 9.05).

To determine the distance to M31 as well as other parameters of interest we now make use of the sample of Cepheids measured in the near-infrared by Riess et al. (2011), multiple anchors for the Cepheid distance scale, and SN data which can be used to determine the Hubble constant. We follow the same formalism as in Riess et al. (2011), solving one simultaneous system of linear equations which relate Cepheid magnitudes to their absolute magnitudes, slope of their P–L relations, local metallicity, distances to their hosts, and –with the inclusion of SN Ia data– a measurement of the Hubble constant. The Cepheids of M31 are assumed to share the same nuisance parameters as other Cepheids (i.e., luminosity, slope of P–L , metallicity dependence) but with a unique distance. For the M31 Cepheids, the photometric system used to measure their colors was somewhat different. While the Cepheids in the 8 SN Ia hosts, the maser host NGC 4258, and M31 were all measured with $F160W$ on WFC3-IR, the optical colors of the POMME M31 Cepheids, useful for dereddening, were not measured by Megacam or PHAT with the same V and I bands on HST as the others. To account for this difference we employed one of two different prescriptions: 1) we assumed a uniform value for the $V - I$ color of the M31 Cepheids as the mean of those measured from the ground by the DIRECT program, $V - I = 1.23 \pm 0.03$, (indicated as fit $PLW = H_{V,I}$ in Table 3); or 2) we used the individual $F110W - F160W$ colors measured for the M31 Cepheids from the PHAT data with a small offset derived to give the same mean color correction in $V - I$ from DIRECT[1] (indicated as $PLW = H_{J,H,X}$ in Table 3). The advantage of the latter approach is that it can account for *differential* reddening along the line of sight while providing a reddening correction which is consistent with that used for non-M31 Cepheids. We adopt an 0.03 mag systematic uncertainty for the use of colors measured with a different photometric system and an 0.04 mag systematic uncertainty between near-IR magnitudes of Cepheids measured on the ground and those measured from space.

[1]By equating the mean $V - I$ dereddening with that for $F110W - F160W$ we can solve for a color offset to insure they have the same mean. That is, $0.504 < V - I >= 1.54 < F110W - F160W - X >$, where $< V - I >$=1.23, gives $X = -0.066$ mag.

Table 3. Global Fits

#	χ^2_{dof}	μ_{M31}	N	H_0	<P	[O/H][a]	$\delta M/\delta$[O/H]	b	Scale	PLW	R_V
1	0.92	**24.415(0.052)**	514	**73.60(2.35)**	Y	zkh	-0.09(0.09)	-3.21(0.03)	4258+MW+LMC	$H_{J,H,X}$	3.1
2	0.92	24.403(0.050)	514	73.54(2.35)	Y	zkh	——	-3.21(0.03)	4258+MW+LMC	$H_{J,H,X}$	3.1
3	0.79	24.421(0.048)	514	74.06(2.20)	Y	zkh	-0.13(0.09)	-3.19(0.02)	4258+MW+LMC	$H_{V,I}$	3.1
4	0.79	24.402(0.047)	514	73.97(2.20)	Y	zkh	——	-3.19(0.02)	4258+MW+LMC	$H_{V,I}$	3.1
5	0.89	24.568(0.046)	553	74.40(2.28)	Y	zkh	-0.12(0.09)	-3.08(0.02)	4258+MW+LMC	H	3.1
6	0.86	24.438(0.049)	514	73.99(2.29)	Y	zkh	-0.10(0.09)	-3.19(0.03)	4258+MW+LMC	$H_{J,H,X}$	2.5
7	1.88	24.413(0.074)	636	74.87(3.32)	Y	zkh	-0.09(0.13)	-3.17(0.04)	4258+MW+LMC	$H_{J,H,X}$	3.1
8	0.89	24.410(0.051)	563	74.66(2.32)	N	zkh	-0.08(0.09)	-3.20(0.03)	4258+MW+LMC	$H_{J,H,X}$	3.1
9	0.92	24.400(0.051)	514	73.98(2.46)	Y	T_e	-0.09(0.13)	-3.21(0.03)	4258+MW+LMC	$H_{J,H,X}$	3.1
10	0.84	24.468(0.070)	448	73.78(3.11)	Y	zkh	-0.20(0.11)	-3.11(0.06)	4258	$H_{J,H,X}$	3.1
11	0.91	24.380(0.064)	514	75.39(2.87)	Y	zkh	-0.18(0.12)	-3.20(0.03)	MW	$H_{J,H,X}$	3.1
12	0.90	24.500(0.098)	514	71.41(3.41)	Y	zkh	-0.18(0.11)	-3.20(0.03)	LMC	$H_{J,H,X}$	3.1
13	0.92	— (—)	514	74.00(2.25)	Y	zkh	-0.08(0.09)	-3.21(0.03)	4258+MW+LMC+M31	$H_{J,H,X}$	3.1
14	0.90	— (—)	514	76.17(3.62)	Y	zkh	-0.18(0.11)	-3.20(0.03)	M31	$H_{J,H,X}$	3.1

[a] Note: metallicity calibration reference: zkh: Zaritsky et al. (1994), T_e: Bresolin (2011).

Our best distance estimate for M31 is $\mu_0 = 24.415 \pm 0.052$, a 2.4% (statistical) distance determination which makes use of independent distance determinations to NGC 4258, Milky Way Cepheid parallaxes, and DEB distances in the LMC (see Riess et al. 2011, for a description of these distance-scale anchors).

The best fit parameters are given in Table 3, top line. Column 2 gives the value of χ^2_{dof}, Column 3 the distance modulus of M31 and its statistical uncertainty, Column 4 the number of Cepheids used in the fit, Column 5 the value and total uncertainty in H_0, Column 6 is a flag to indicate the use of Cepheids below the optical completeness limit (see below), Column 7 gives the metallicity calibration used, Column 8 the correlation coefficient in the PLWZ regression, Column 9 the value and uncertainty of the slope of the Cepheid PLWZ relation. The next three columns are used to indicate variants in the analysis whose impact we now consider.

Ignoring the metallicity parameter (lines 2 and 4), changing the method of color correction (line 3), changing the reddening parameter for the Cepheids from $R_V = 3.1$ to $R_V = 2.5$ (line 6), or changing the metallicity scale from Zaritsky et al. (1994) to that of Bresolin (2011) (line 8), changes the distance to M31 by < 0.02 mag. Failing to clip outliers in any Cepheid P–L relations (line 7) doubles the χ^2_{dof} but changes the distance to M31 by < 0.01 mag. Retaining infrared measurements of Cepheids with periods below the optically-determined completeness limit (indicated by $< P = N$, line 8), has no effect on the distance. The only significant change in the distance to M31 occurs when discarding the color measurements used to account for extinction (line 5). The 0.15 mag increase in the distance in this case indicates that the M31 Cepheids have *more* extinction, $\Delta A_H = 0.15$ mag (or $DeltaA_V = 0.75$ mag) than the average of the mostly extragalactic Cepheids in other hosts. This is not surprising as M31 is more inclined than any of the other hosts. We also used each of the 3 distance-scale anchors separately as shown in lines 10 to 12. The uncertainties in the distances increase with the use of only a single anchor. The lowest uncertainty is from the use of the parallax measurements by Benedict et al. (2007) to Milky Way Cepheids (line 11), resulting in $\mu_0 = 24.38 \pm 0.064$.

Following the approach of Riess et al. (2011), we quantify the *systematic* uncertainty in the distance to M31 from the dispersion of the variants in the analysis, $\sigma = 0.03$ mag for the 12 variants not including the one neglecting color information which ignores the large extinction for the M31 Cepheids due to inclination. Thus our best estimate of the distance to M31 is $\mu_0 = 24.42 \pm 0.05 \pm 0.03$ or 765 ± 28 kpc. This distance is in excellent agreement with the frequently-cited measurement from Freedman & Madore (1990) and sits near the middle of the range of past measurements summarized by McConnachie et al. (2005).

Lastly, we made use of the two DEB measurements for M31 from Ribas et al. (2005) and Vilardell et al. (2010) with a mean of $\mu_0 = 24.36 \pm 0.08$ to determine the Hubble constant by their ability to calibrate the Cepheid luminosities. Combined with the preceding three anchors (line 13), the use of the independent M31 distance has negligible impact, increasing the Hubble constant by 0.2 km s^{-1} Mpc^{-1} to 74.0 km s^{-1} Mpc^{-1} with no reduction in uncertainty. The present limitations

of the use of M31 as an independent anchor are the lack of $V-I$ colors measured with HST WFC3 and the lower precision of its independent distance compared to the other 3 anchors. The use of M31 DEB results without any of the other anchors (line 14) yields a larger Hubble constant with larger error though still consistent with prior results. The best fit to the Hubble constant (line 1), which only makes use of the M31 Cepheids to constrain the slope and metallicity parameter, is 73.6 ± 2.4 km s^{-1} Mpc^{-1} and does not bring a significant difference to the one inferred by Riess et al. (2011).

3. Discussion

The main advantages of the PHAT space-based observations of Cepheids presented here over previous data come from the reduction in extinction and crowding. The result is the tightest P–L relation for M31 Cepheids yet seen, which, combined with past, external calibrations, yields the most precise distance measurement for M31. The improved precision over the past history of optical, ground-based P–L relations is striking and continues to indicate the value of this kind of data for measuring the Hubble constant and dark energy (Riess et al. 2011).

To see more clearly the advantages of these spaced-based observations over those from the ground we simulated the effect of crowding for near-infrared Cepheid magnitudes obtained with good ground-based seeing by measuring the flux contained in an aperture of radius r=0.″9. The dispersion increased from 0.20 to 0.24 mag in $F110W$, the slope of the P–L relation flattened by 0.5 and the intercept became brighter by 0.3 mag. This is not unexpected as the impact of crowding is greater for the lower-period, fainter Cepheids. These results are similar to those determined for ground-based crowding in the optical by Mochejska et al. (2000). It is important to note that the effect of crowding is far more severe for M31 due to its large inclination than for less inclined galaxies, even those much farther away. In addition, Cepheids found from the ground via image subtraction are likely to suffer significantly *greater* crowding than those selected from PSF fitting as the addition of comparable constant flux to a PSF fit will reduce the amplitude of the light curve and remove the object from an amplitude-selected sample (Ferrarese et al. 2000).

The P–L relations for M31 may still improve in the near future. Additional observations by the PHAT program should augment the Cepheid sample by dozens. Cepheids with $\log P < 1$, though less useful for distance scale work, can be mined from the data to study the short period end of the relation. The use of Cepheid phase information from concurrent, ground-based optical monitoring of M31 can be used to recover the phase of the PHAT observations, reducing the scatter of the P–L by up to $\sim 50\%$, an equivalent leverage as doubling the sample of measurements presented here.

We are grateful to the members of the PHAT MCT Program led by Julianne Dalcanton and aided by Jason Kalirai for their tremendous efforts to obtain the PHAT measurements and their support of this work. Financial support for this work was provided in part by the POMMME project (ANR 09-BLAN-0228). This work is also based on observations obtained with

MegaPrime/MegaCam, a joint project of CFHT and CEA/DAPNIA, at the CFHT which is operated by the National Research Council (NRC) of Canada, the Institut National des Sciences de l'Univers of the Centre National de la Recherche Scientifique (CNRS) of France, and the University of Hawaii. JF acknowledges the hospitality of GEPI, where part of the POMME work was carried out.

Facilities: HST, CFHT

REFERENCES

An, J. H., et al. 2004, MNRAS, 351, 1071

Baade, W., & Swope, H. H. 1963, AJ, 68, 435

—. 1965, AJ, 70, 212

Benedict, G. F., et al. 2007, AJ, 133, 1810

Bonanos, A. Z., Stanek, K. Z., Sasselov, D. D., Mochejska, B. J., Macri, L. M., & Kaluzny, J. 2003, AJ, 126, 175

Bresolin, F. 2011, ApJ, 729, 56

Brown, T. M., Smith, E., Guhathakurta, P., Rich, R. M., Ferguson, H. C., Renzini, A., Sweigart, A. V., & Kimble, R. A. 2006, ApJ, 636, L89

Cardelli, J. A., Clayton, G. C., & Mathis, J. S. 1989, ApJ, 345, 245

Clerke, A. 1903, Problems in astrophysics (London: A. & C. Black)

Dalcanton, J., & et al. 2012, to be submitted

De Vaucouleurs, G., & Corwin, Jr., H. G. 1985, ApJ, 295, 287

Ferrarese, L., Silbermann, N. A., Mould, J. R., Stetson, P. B., Saha, A., Freedman, W. L., & Kennicutt, Jr., R. C. 2000, PASP, 112, 177

Fliri, J., Riffeser, A., Seitz, S., & Bender, R. 2006, A&A, 445, 423

Fliri, J., Valls-Gabaud, D., & Magnier, E. A. 2012, to be submitted

Freedman, W. L., & Madore, B. F. 1990, ApJ, 365, 186

Hubble, E. P. 1929, ApJ, 69, 103

Lee, C.-H., et al. 2011, ArXiv e-prints http://arxiv.org/abs/1109.6320

Macri, L. M., et al. 2001, ApJ, 549, 721

Madore, B. F., & Freedman, W. L. 1991, PASP, 103, 933

Magnier, E. A., Augusteijn, T., Prins, S., van Paradijs, J., & Lewin, W. H. G. 1997, A&AS, 126, 401

McConnachie, A. W., Irwin, M. J., Ferguson, A. M. N., Ibata, R. A., Lewis, G. F., & Tanvir, N. 2005, MNRAS, 356, 979

Mochejska, B. J., Macri, L. M., Sasselov, D. D., & Stanek, K. Z. 2000, AJ, 120, 810

Persson, S. E., Madore, B. F., Krzemiński, W., Freedman, W. L., Roth, M., & Murphy, D. C. 2004, AJ, 128, 2239

Ribas, I., Jordi, C., Vilardell, F., Fitzpatrick, E. L., Hilditch, R. W., & Guinan, E. F. 2005, ApJ, 635, L37

Riess, A. G., et al. 2011, ApJ, 730, 119

Vilardell, F., Jordi, C., & Ribas, I. 2007, A&A, 473, 847

Vilardell, F., Ribas, I., Jordi, C., Fitzpatrick, E. L., & Guinan, E. F. 2010, A&A, 509, A70

Zaritsky, D., Kennicutt, Jr., R. C., & Huchra, J. P. 1994, ApJ, 420, 87

This preprint was prepared with the AAS LaTeX macros v5.2.

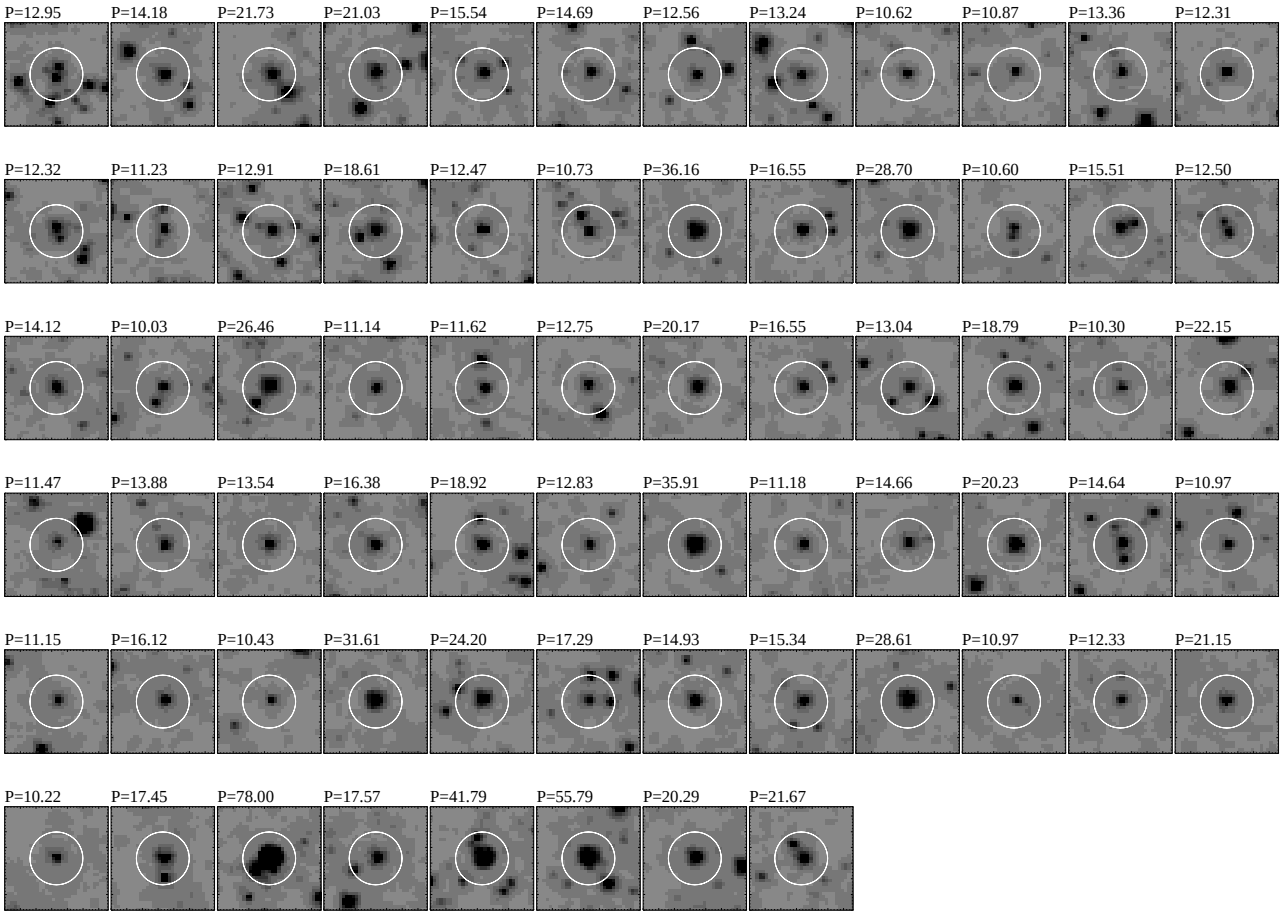

Fig. 1.— HST near-IR $F160W$ images of 68 Cepheids in M31 (ordered as in Table 1), spanning nearly an order of magnitude in period. The scale of each stamp is $2.5''$(32 pixels). The position of the Cepheid as determined from the optical Megacam POMME images in indicated by the circle, which has a diameter of $1''$.

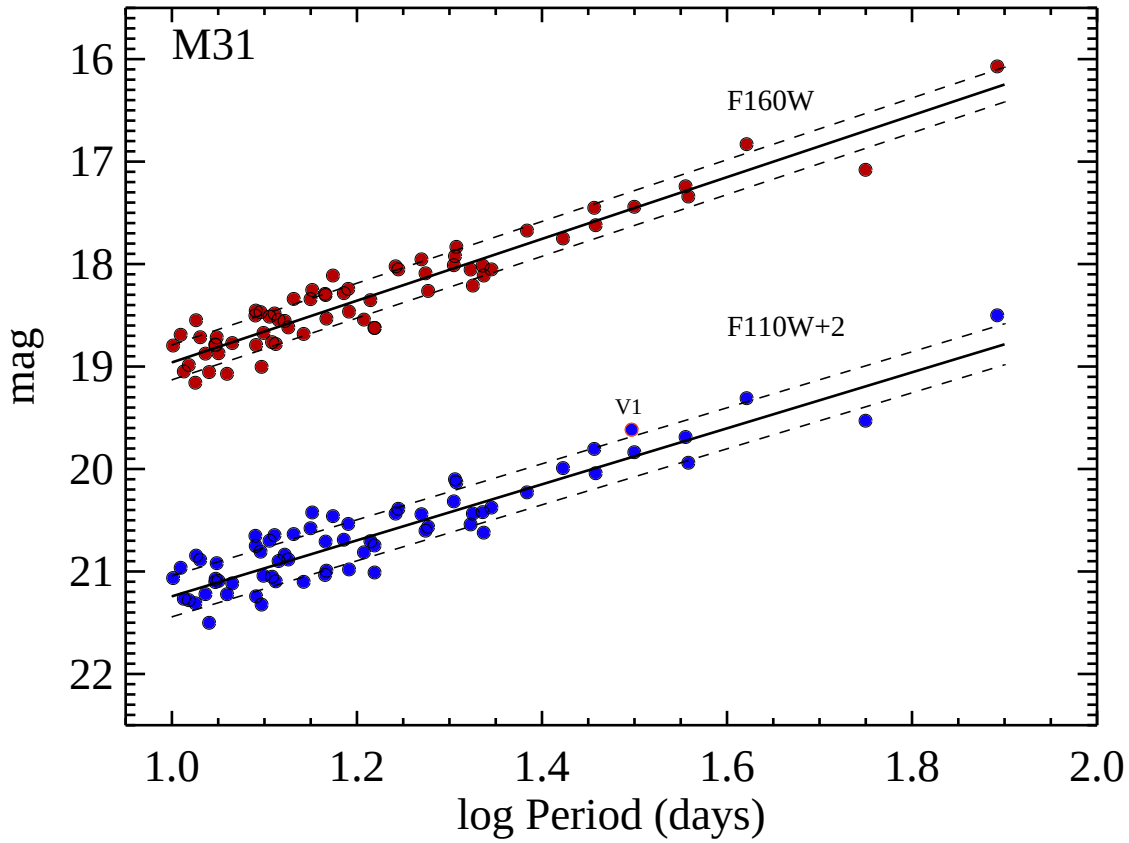

Fig. 2.— Near-IR P–L relations for 69 Cepheids in M31 with $\log P > 1$ (Table 1). The single slope fitted to the relations is given in Table 2, and is shown as the solid lines. Dashed lines indicate the average dispersion of 0.17 mag ($F160W$), a factor 3.5 smaller than previous ground-based optical P–L relations, and 0.20 mag ($F110W$).